ELSEVIER

Journal of Chromatography B, 743 (2000) 169–180

JOURNAL OF CHROMATOGRAPHY B

www.elsevier.com/locate/chromb

Partitioning and diffusion of large molecules in fibrous structures

J.C. Bosma*, J.A. Wesselingh

Department of Chemical Engineering, University of Groningen, Nijenborgh 4, 9747 AG Groningen, The Netherlands

Abstract

This paper consists of three parts. In the first part we present diffusion and partition coefficients of proteins in agarose that were measured with gel permeation chromatography. In the second part we present a partition model which includes the effects of solute concentration and of cosolutes. In the third part we modify and extend Ogston's diffusion equation to account for the effects of solute and fiber flexibility, solute concentration and cosolutes. We find good agreement between the proposed models and data from the literature.

Keywords: Partitioning; Diffusion; Proteins; Polymers

1. General introduction

Partitioning and diffusion of large molecules in fibrous structures is important in several applications such as gel permeation chromatography, controlled drug release, ultrafiltration and electrophoresis. In this paper we examine these phenomena in three parts. In the first part we present measurements with gel permeation chromatography. In the second part we present a new partition model of which Ogston's partition equation is a limiting case. In the third part we present an extension of Ogston's diffusion model and a comparison of Ogston's partition and diffusion models with data collected from the literature. The extensions that we propose include the effects of solute and fiber flexibility, of solute concentration and of cosolutes. The new equations are not restricted to systems with fibrous structures but can be applied to systems with relatively large elements, such as two phase systems with proteins and micelles or biological systems such as blood.

2. PART 1. Chromatographic measurement

2.1. Introduction

Diffusion and partition coefficients of proteins in gels can be measured by various methods, among them are ultrafiltration, fluorescence recovery after photobleaching and gel permeation chromatography (GPC). In GPC the retention time of a peak depends on the partition coefficient of the protein in the gel. The peak broadness depends, among other things, on the diffusion coefficient of the protein in the gel. In order to extract these coefficients from the experimental data a model is needed to describe the process taking place in the column. Chromatography is a commonly used technique for measuring partitioning and diffusion coefficients; it is not restricted

*Corresponding author. Tel.: +31-50-363-7241; fax: +31-50-363-4479.

E-mail address: j.c.bosma@chem.rug.nl (J.C. Bosma)

0378-4347/00/$ – see front matter
PII: S0378-4347(00)00134-1

to gel permeation chromatography. The experimental procedures and the models that are used differ slightly from author to author. Here we present our model and our measurements of partition and diffusion coefficients of proteins in a gel with ion-exchange groups, under non-binding conditions.

2.2. Experimental method

Q-Sepharose FF is an agarose based ion-exchange gel that was obtained from Pharmacia Biotech (Uppsala, Sweden), it has a mean particle diameter of 96 μm. Bovine serum albumin (BSA) was obtained from Boehringer Mannheim (now a part of Roche, Basel, Switzerland) (735108), other proteins were obtained from Sigma Chemicals (Zwijndrecht, The Netherlands): ovalbumin (A5503), cytochrome *c* (C2037), lysozyme (L6876) and γ-globulin (G5009). Important parameters of these substances can be found in Table 1. The experiments were performed on an FPLC system from Pharmacia Biotech which included an XK16 column (1.58 cm ID, 10.55 cm bed length), a V7 valve for sample injection, a P500 pump, a UV-MII UV monitor and a conductivity monitor (18-1104-39). The experiments were performed at room temperature (22°C).

We performed pulse response measurements with these proteins in the Q-Sepharose FF column. In order to measure the effect of axial dispersion on the peak broadness we also performed experiments with sodium chloride pulses. The buffer that we used for elution and for dissolving the proteins was an acetic acid/acetate buffer with an acetate concentration of 1 mol/l and a pH of 4.4. In this buffer no binding of the proteins to the adsorbent occurred. The pulses were introduced into the feed of the column with an injection valve and an injection loop of 0.5 ml. The protein concentration in the injected pulses was 10 g/l. In the experiments with sodium chloride we used an elution buffer with 0.02 mol/l sodium chloride and a pulse with 1 mol/l sodium chloride. The flow through the column was varied between 0.1 and 4 ml/min. At the outlet of the column the conductivity and the UV-adsorption at 280 nm were measured.

In a typical experiment the buffer was continuously passed through the column. Then the injection loop was filled with the protein solution and the injection valve was switched to introduce the pulse into the feed. Finally the elution profile was measured at the outlet of the column.

Table 1
Parameters in and results of the gel permeation experiments. The molecular weights and diffusion coefficients were obtained from [1] and [2], the Stokes radii were calculated from the diffusion coefficients with: $r_{\text{Stokes}} = RT/6\pi N_A \eta D_0$

Species	M_m [g/mol]	$10^{12}D_0$ [m²/s]	r_{Stokes} [Å]	K [–]	D/D_0 [–]
NaCl	58.5	1610		0.86	0.53
Cytochrome *c*	12 300	130	16.6	0.64	0.21
Lysozyme	14 300	113	19.1	0.63	0.22
Ovalbumin	43 500	73	29.6	0.62	0.18
BSA	66 270	59	36.6	0.59	0.16
γ-globulin	169 000	41	52.7	0.47	0.15

2.3. Modeling

We assumed that the column could be represented by a large number of tanks in series with each ''tank'' consisting of an ideally mixed mobile liquid part with holdup ε_l and an ideally mixed stagnant part. Mass transfer was modeled with the Linear Driving Force (LDF) model; it was shown by Vonk [3] that this works well for gel permeation chromatography modeling. In the LDF model it is assumed that mass transfer occurs through two films in series: the liquid film with mass transfer resistance $1/k_l$, and the particle film with resistance $1/k_p$. The mass balance for the two parts of each ''tank'' then becomes:

$$
\begin{aligned}
&\frac{\partial c}{\partial t} = -\frac{1-\varepsilon_l}{\varepsilon_l} MT + \frac{\nu_{\text{sup}}}{\varepsilon_l L_{\text{tank}}}(c_{\text{in}} - c)\\
&\frac{\partial q}{\partial t} = MT\\
&MT = \frac{6}{d_p}\left(\frac{1}{k_p} + \frac{K}{k_l}\right)^{-1}(Kc - q)\\
&k_p = Sh_p \frac{D}{D_0}\frac{D_0}{d_p}\\
&k_l = Sh_l \frac{D_0}{d_p}\\
&Sh_l = \frac{1.09}{\varepsilon_l}\left(\frac{d_p \nu_{\text{sup}}}{D_0}\right)^{1/3}
\end{aligned}
\qquad (1)
$$

For the Sherwood number on the particle side (Sh_p) we took a value of 10. For the Sherwood number on the liquid side (Sh_l) we used an equation given by Wilson and Geankoplis [4]. The equation given by Pfeffer [5] is similar and gives almost the same results. In the case of proteins the main resistance to mass transfer is located in the particle film.

2.4. Results and discussion

We did not succeed in measuring the mobile liquid holdup in the column, therefore we assumed a value of 0.37. The number of tanks is representative for the axial dispersion. To calculate this number we used the extrapolated point (♦) at zero velocity in Fig. 3, at this point the peak broadness is thought to be only affected by axial dispersion. We found a number of 275 tanks. With a bed length of 10.55 cm and a particle diameter of 96 μm this gives each tank a length of about 4 particle diameters.

The partition coefficient, K, of each solute was fitted with the breakthrough time of the peaks; the retardation coefficient, D/D_0, was fitted with the peak broadness. The results of the experiments can be found in Figs. 1–3 and Table 1.

The value for D/D_0 for NaCl may seem a little small but there is a large uncertainty in this value because the broadness of the salt peaks depends almost solely on axial dispersion. With regard to the peak shape (skewness) there was good agreement between the measurements and the simulations as can be seen in Fig. 1. The peaks in Fig. 1 are at the highest liquid velocity and they show the largest difference between the measurements and the model predictions.

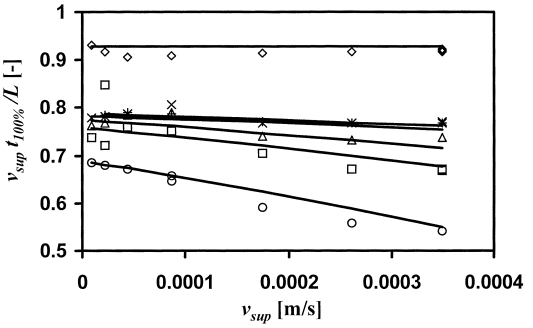

Fig. 2. Measured and calculated breakthrough times of the top of the peaks (for definition of symbols see Fig. 1).

3. PART 2. Extension of Ogston's partition model

3.1. Introduction

The partitioning of large solutes between fibrous structures and the surrounding liquid is generally described with Ogston's partition model [6]. However, as we will show, the way other authors introduced the fiber holdup into this model can be improved. Also, the model is only valid at low solute concentrations. Not much is known about the effect of concentration on the partitioning. Fanti and Glandt [7] give an expression that correlated well with their Monte Carlo simulations. This equation is strictly only valid for very thin fibers.

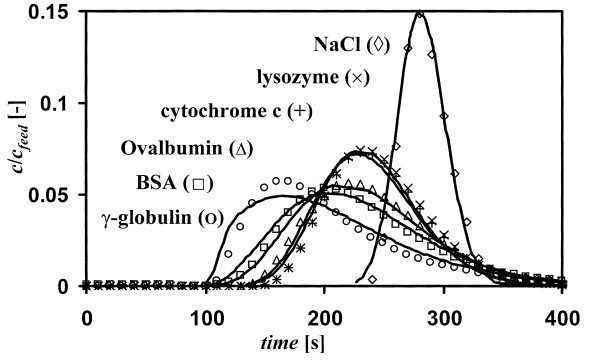

Fig. 1. Measured (points) and calculated (lines) eluted peaks at $v_{sup} = 0.35$ mm/s.

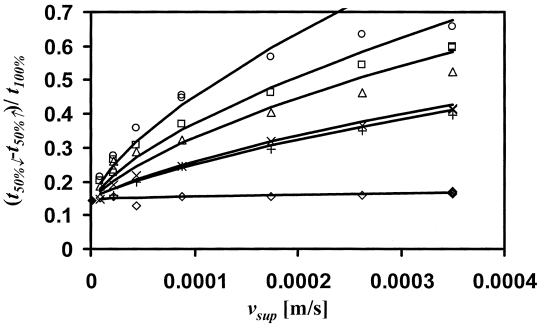

Fig. 3. Measured and calculated peak broadness (for definition of symbols see Fig. 1).

In this section we first derive a variation of Ogston's equation which does give the influence of the fiber holdup correctly. Then we show a new way of deriving Ogston's equation. Finally we extend the new model to account for higher solute concentrations and the effect of cosolutes.

3.2. Introducing the fiber holdup into Ogston's model in a correct way

In 1958 Ogston derived a model for the partitioning of large molecules in fibrous structures [6]. In this model he assumes that a gel consists of randomly oriented infinitely thin and infinitely long fibers; the solutes are taken to be rigid spheres. The equation that Ogston derived for the partition coefficient can be written as:

$$K = \mathrm{e}^{-\alpha} \tag{2}$$

with

$$\alpha = \pi l r_s^2 \tag{3}$$

where l is the fiber length per volume and r_s is the solute radius. When the fibers are not infinitely thin the dimensionless number α is usually rewritten as:

$$\alpha = \phi \left(1 + \frac{r_s}{r_f}\right)^2 \tag{4}$$

where r_f is the fiber radius and ϕ is the fiber holdup. In the derivation of this formula it is assumed that the fibers do not overlap. However this formula is not exact, because for very small solutes the partition coefficient should be $1-\phi$ instead of $\exp(-\phi)$. Here we show how the fiber holdup can be incorporated correctly in the dimensionless number α.

Ogston assumes that the fibers are infinitely thin, and so he can neglect any overlap of the fibers. In real gels fibers that have a certain thickness and can overlap better represent the structure. Then the overlap cannot be neglected and a better form of the parameter α appears to be:

$$\alpha = f \left(1 + \frac{r_s}{r_f}\right)^2 \tag{5}$$

where f is the fiber holdup including overlapping fibers (which means f can be larger than 1).

We need a relation between f and ϕ and we find it with a cell model. Suppose the gel can be represented by P equally sized cells. We begin with P empty cells, and begin to add fiber elements to these at random, until the fraction ϕ is filled with fiber. During this filling we count two numbers:

1. In the first count we allow each cell to be counted any number of times. A cell filled twice represents an overlap of two fibers. This count is related to f, the fraction of fibers including overlap.
2. In the second count, a filled cell cannot be counted a second time. This count is related to ϕ, the fiber volume fraction without fiber overlap.

The first cell encountered is always empty, therefore the number of filled cells according to the second count begins with:

$$N_1 = 1 \tag{6}$$

where the subscript is the number of filled cells according to the first count. Every further time a cell is filled we have for the second count:

$$N_{i+1} = N_i + \left(1 - \frac{N_i}{P}\right) \tag{7}$$

The second term on the right hand is the chance that the cell is still empty. Eq. (7) can easily be extended. For example, using it three times gives:

$$N_{i+1} = 1 + \left(1 - \frac{1}{P}\right) + \left(1 - \frac{1}{P}\right)^2 + \left(1 - \frac{1}{P}\right)^3 + \left(1 - \frac{1}{P}\right)^4 N_{i-3} \tag{8}$$

This can be extended and then solved to give:

$$N_F = \sum_{i=0}^{F-1} \left(1 - \frac{1}{P}\right)^i = P\left\{1 - \left(1 - \frac{1}{P}\right)^F\right\} \tag{9}$$

For a large number of cells this yields:

$$\phi = \lim_{P\to\infty} \frac{N_F}{P} = \lim_{P\to\infty} \left[1 - \left(1 - \frac{1}{P}\right)^{fP}\right] = \frac{\mathrm{e}^f - 1}{\mathrm{e}^f} \tag{10}$$

where we made use of $F = fP$ and $N_F = \phi P$. This can be rearranged as:

$$f = \ln\left(\frac{1}{1-\phi}\right) \tag{11}$$

The result for the partition coefficient is:

$$K = (1-\phi)^{(1+(r_s/r_f))^2} \tag{12}$$

This equation does have the correct limiting behavior for small solutes. The difference between this equation and the original Ogston equation becomes important for large values of the volume fraction ϕ of the fibers.

3.3. A new derivation of Ogston's partition equation

The method used above of relating the fiber holdup, ϕ, to the fiber holdup including overlapping fibers, f, also offers a way to derive Ogston's partition equation. Consider the process of increasing the fiber radius and decreasing the solute radius to zero, keeping their sum constant. During this process the partition coefficient will be constant and at the end it will equal $1-\phi'$. Here ϕ' is the fiber holdup without overlapping fibers extrapolated to zero solute radius; this can also be called the excluded volume. This ϕ' is related to an f', the excluded volume including overlapping fibers, in the same way as ϕ and f are related (Eqs. (10) or (11)). The fs are proportional to the square of the fiber radius, which gives:

$$f' = f\left(\frac{r_f + r_s}{r_f}\right)^2 \tag{13}$$

With these relations we find:

$$K = 1-\phi' = \exp(-f') = \exp\left(-f\left(1+\frac{r_s}{r_f}\right)^2\right)$$
$$= (1-\phi)^{(1+(r_s/r_f))^2} \tag{14}$$

This is the same result as found before.

3.4. Extending the new partition model

The method used above can easily be extended to include higher solute concentrations and the effect of cosolutes. In order to do this we first consider the relation between the partitioning and the excluded volumes in the gel and in the bulk.

An expression for the partitioning equilibrium can be derived in the same way as the common Langmuir equation for adsorption equilibrium. At equilibrium the rate at which the solute goes from the bulk to the gel should be equal to the rate at which it goes the other way. We assume that the rate is proportional to the volume fraction of the solute in the phase where it comes from and to the available volume in the phase where it goes to. The available volume is the volume in a phase available for the center of the solute divided by the total volume of that phase: it equals one minus the excluded volume. This gives:

$$k\phi_{i,b}(1-\phi'_i) = k\phi_i(1-\phi'_{i,b}) \tag{15}$$

where k is a rate coefficient, ϕ_i and $\phi_{i,b}$ are the solute holdup in the gel and the bulk and ϕ'_i and $\phi'_{i,b}$ are the excluded volume in the gel and the bulk. For the partition coefficient this gives:

$$K = \frac{\phi_i}{\phi_{i,b}} = \frac{1-\phi'_i}{1-\phi'_{i,b}} \tag{16}$$

So the problem is reduced to finding the excluded volumes in both phases. We calculate these in four steps:

1. First we calculate the total holdup, ϕ_{tot}, of all objects that can exclude a solute (these include the solute itself).
2. From this we calculate the total holdup including overlap, f_{tot}, with Eq. (11).
3. From this we calculate for a certain component i the excluded volume including overlap, f'_i,
4. And from this we calculate the real excluded volume, ϕ'_i, with Eq. (11).

In the third step we need a relation between f' and f: the ratio of f' and f is the ratio of the volume excluded by a single object and the real volume of that object. For a sphere between fibers it is given by Eq. (13). For a sphere with radius r_i between other spheres with radius r_j it becomes:

$$f' = f\left(\frac{r_i + r_j}{r_j}\right)^3 \tag{17}$$

because the volume of a sphere is proportional to the

third power of the radius. For a sphere between equal spheres it becomes:

$$f' = 8f \tag{18}$$

For a sphere between fibers, other spheres and like spheres we use an interpolation:

$$f' = f\,\frac{\left(\frac{r_i + r_f}{r_f}\right)^2 \phi_f + 8\phi_i + \sum_j \left(\frac{r_i + r_j}{r_j}\right)^3 \phi_j}{\phi_f + \phi_i + \sum_j \phi_j} \tag{19}$$

Finally we find a set of implicit equations for the partition coefficients:

$$\frac{1}{\phi_{i,b}} \exp\left[\frac{8\phi_{i,b} + \sum_j \left(\frac{r_i + r_j}{r_j}\right)^3 \phi_{j,b}}{\phi_{i,b} + \sum_i \phi_{j,b}} \times \ln\left(1 - \phi_{i,b} - \sum_j \phi_{j,b}\right)\right]$$

$$= \frac{1}{\phi_i} \exp\left[\frac{\left(\frac{r_i + r_f}{r_f}\right)^2 \phi_f + 8\phi_i + \sum_j \left(\frac{r_i + r_j}{r_j}\right)^3 \phi_j}{\phi_f + \phi_i + \sum_j \phi_j} \times \ln\left(1 - \phi_f - \phi_i - \sum_j \phi_j\right)\right] \tag{20}$$

where subscript b denotes the bulk phase. The partition coefficients can be calculated with the first part of Eq. (16) after the set of Eqs. (20) have been solved simultaneously for all solutes that are able to partition between the gel and the bulk.

3.5. Discussion

The interpolation in Eq. (19) is not exact, therefore we have to test the equation for some limiting cases. When there are no cosolutes and the solute concentration is low, Eq. (20) reduces to Ogston's equation, as it should. When there are no cosolutes and the fiber radius is very small the results of Eq. (20) can be compared to those that Fanti and Glandt [7] obtained with Monte Carlo simulations. This is done in Fig. 4, it is seen that the agreement is quite good. Therefore we think that the model gives a reasonable estimation of the partition coefficient. The model is also very flexible, for instance for a sphere between short fibers with length l_f we can use:

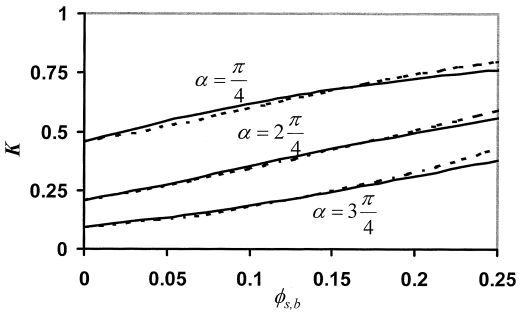

Fig. 4. Comparison of Eq. (20) (solid lines) with the results of Fanti and Glandt [7] (broken lines).

$$f' = f\,\frac{(r_f + r_s)^2 (l_f + 2r_s)}{r_f^2 l_f} \tag{21}$$

And for a sphere between (randomly distributed) flat plates with surface A, circumference C and thickness d we can use:

$$f' = f\,\frac{(A + Cr_s)(d + 2r_s)}{Ad} \tag{22}$$

These equations can be introduced into Eq. (19) in the same way as Eqs. (17) and (18) were introduced.

4. PART 3. Extension of Ogston's diffusion model and comparison with experimental data

4.1. Introduction

Various models are used for the estimation of diffusion coefficients in fibrous structures (see e.g. [8–11]). Usually the models give an estimation for the retardation of the solute by the gel, this is the ratio of the diffusion coefficient in the fibrous structure and the diffusion coefficient in free solution (D/D_0). The most well-known models are Ogston's diffusion model [11] and the effective medium model [12]. Ogston's model takes the effect of the

fiber radius, the solute radius and the fiber holdup into account. In the effective medium the effect of the solute radius and the gel permeability are taken into account.

In this section of the paper we present some data collected from the literature. Based on this data we propose two modifications of Ogston's diffusion model [11]: the introduction of flexibility factors of the solute and the fiber and of two diffusion regimes. In order to compare Ogston's diffusion model with experimental data we need reliable values for the fiber thicknesses. We derive these from a comparison of Ogston's partition model with the experimental data.

Finally we propose an extension of the diffusion equation to systems with higher solute concentrations and cosolutes.

4.2. Comparison of Ogston's models with data from the literature

In this section we compare Ogston's partition and diffusion models with experimental results from ourselves and from others. Table 2 gives an overview of the sources of the collected data. We arranged the data in groups according to the nature of the fibers (agarose, sephadex or polyacrylamide) and the solutes (protein, linear polymer or virus).

Ogston's model is given by Eq. (2) with:

Table 2
Overview of sources of collected data, system abbreviations are: Po: linear polymer; Pr: protein; MV: Southern Bean Mosaic Virus; A: agarose; S: Sephadex; P or PAA: polyacrylamide

Data source	System	Technique	Comments
Poitevin and Wahl [13]	Dextrans in Sephadex (Po–S)	FRAP	[a]
Moussaoui et al. [14]	Proteins in AcA-34 (Pr–P)	FRAP	AcA-34 consists of 4% agarose and 3% PAA, we assumed that only the 3% PAA was present
Moussaoui et al. [15]	Proteins in Sepharose Cl–B (Pr–A)	FRAP	
Johnson et al. [16]	Proteins in SP-Sepharose (Pr–A)	FRAP	
Johnson et al. [17]	Proteins and Ficolls in agarose (Pr–A, Po–A)	FRAP	[b]
Tong and Andersson [18]	Proteins and PEGs in PAA (Pr–P, Po–P)	FRAP	
Ackers and Steere [19]	Proteins and Mosaic Virus in Agar (Pr–A, MV–A)	Ultrafiltration	[b], actually $K/K_{salt} \cdot D/D_0$ was measured; we assumed that agar has the same properties as agarose
Williams et al. [9]	Dextrans in PAA (Po–P)	Ultrafiltration	
Laurent and Killander [20]	Dextrans in Sephadex (Po–S)	Chromatography	Only *K*s were measured
Boyer and Hsu [21]	Proteins in Sepharose Cl-6B (Pr–A)	Chromatography	
Vonk [3]	Proteins in Sephadex (Pr–S)	Chromatography	
Present study	Proteins in Q-Sepharose FF (Pr–A)	Chromatography	

[a] The measurements of Poitevin and Wahl [13] do not agree with those of others [3,20]. We have assumed that the authors estimated the Stokes radii of the dextrans a factor 1.5 too high and have used corrected Stokes radii in our calculations. We think they made an error with the Stokes radii because these were estimated in a complicated way, while the other parameters (K and D/D_0) follow quite straightforward from the experiments.

[b] K was not measured, we estimated it with Eq. (2).

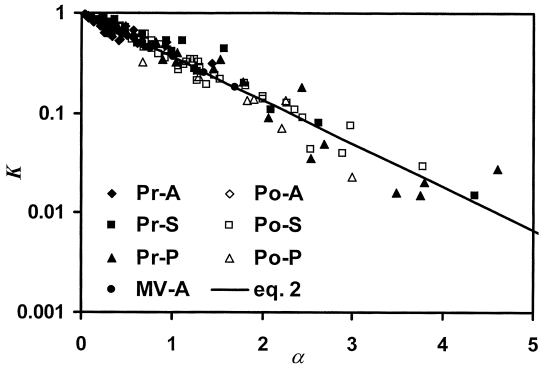

Fig. 5. The fit of Ogston's partition model (Eq. (2)) (for definition of abbreviations see Table 2).

$$\alpha = \ln\left(\frac{1}{1-\phi}\right)\left(1+\frac{r_s}{r_f}\right)^2 \tag{23}$$

The model works well as can be seen in Fig. 5. In our calculations of the dimensionless number α we used the Stokes radius for the solute radius, r_s; in all cases this radius was given in the publications. For the fiber holdup of Sephadex gels we used the values given by Vonk [3]; for that of Sepharose gels we used the percentage given in the name of the gel, for Sepharose ion-exchange gels we added 2 percent to the solid holdup in order to account for the ion-exchange groups. For the fiber radii, r_f, we used fitted values: for agarose 22 Å, for Sephadex 7.2 Å and for polyacrylamide 6.5 Å. In our opinion these fiber radii do not have much physical significance except that they give good estimations of the size of the holes in fibrous structures. If the fiber radius is unknown α can be calculated from K with Eq. (2); this is possible due to the clear relation between α and K. According to Ogston's diffusion model, which is discussed below, α is also the parameter that determines the retardation, D/D_0. This means that Ogston's diffusion model can also be interpreted as giving a relationship between the partition coefficient and the retardation coefficient.

In 1973 Ogston et al. proposed a model to describe the restricted diffusion of large molecules in fibrous structures [11]. The model is based on Einstein's stochastic model, which assumes that diffusion is a process in which molecules make steps with length λ in a random direction with frequency κ. This gives the following expression for the diffusion coefficient:

$$D = \frac{1}{6}\lambda^2\kappa \tag{24}$$

In a fibrous structure not every step can succeed, if the solute collides with a fiber the step will not succeed. Following Ogston, the probability that a step of length λ can succeed, which equals the retardation, is given by:

$$P_\lambda = \frac{D}{D_0} = \exp\left(-\frac{1}{2}\pi l r \lambda\right) \tag{25}$$

where $\frac{1}{2}\pi lr$ is the average number of collisions per traveled distance. According to Ogston we should choose the step size as limited by the size of the holes in the fibrous structure. The diffusion process is then a process in which solutes jump randomly from one hole to an adjacent hole, with each jump having a certain chance of succeeding. This gives:

$$\lambda = 2/\sqrt{\pi l} \tag{26}$$

And from Eqs. (25) and (26) it follows that:

$$\frac{D}{D_0} = \exp(-\sqrt{\pi l}r) = \exp(-\sqrt{\alpha}) \tag{27}$$

In Fig. 6 this theory is compared with the data we collected. For the sake of consistency we used the

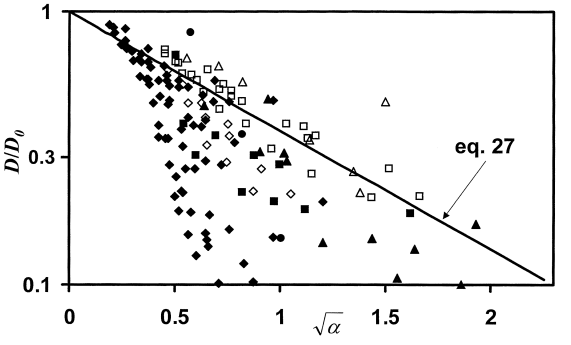

Fig. 6. The fit of Ogston's diffusion model (Eq. (27)) (for definition of symbols see Fig. 5).

same values for the parameters (ϕ, r_f and r_s) as in the calculations for the partition coefficient. As can be seen in Fig. 6 there is considerable scatter in the data and the predictions can be very poor. In the next two sections we propose two modifications to Ogston's diffusion theory which will give better agreement between theory and experiment.

4.3. Incorporating flexibilities into Ogston's diffusion model

As can be seen in Fig. 6, there is considerable scatter in the data, however there are also some clear trends. Linear polymers show consistently higher diffusion coefficients than proteins of the same Stokes radius. Similar differences can be noticed when different fibrous structures are considered. To take this into account we propose the introduction of flexibility factors for the fiber and the solute, f_f and f_s, respectively. If either the solute or the fiber flexibility increases, the chance that a step will succeed will increase. We assume that the average distance traveled up to a collision increases with the flexibility factor. Since Ogston's theory assumes rigid objects we chose to make the flexibility factor for rigid objects unity (we assume that proteins and agarose are rigid). When we incorporated this in Eq. (25) we found (when we compared the new equation with the data) that we still needed an empirical factor of 3. The reason for this is unknown, it might be due to the increased friction between the solute and the solvent which on its turn is caused by the fibers hindering the solvent in its motion. The diffusion coefficient then becomes:

$$\frac{D}{D_0} = \exp\left(\frac{-3r\sqrt{\pi l}}{f_f f_s}\right) = \exp\left(\frac{-3\sqrt{\alpha}}{f_f f_s}\right) \qquad (28)$$

The effect of introducing the flexibility factors can be seen when Figs. 6 and 7 are compared: the consistent differences between the groups have disappeared; the scatter within the groups remains of course. The fitted flexibility factors are given in Table 3. The nature of the flexibility factors is unknown to us, that of the fibers may be related to the fiber radius, r_f, to the real fiber thickness or to the persistence length of the polymer chains, however there is not enough data to state any definite relationship.

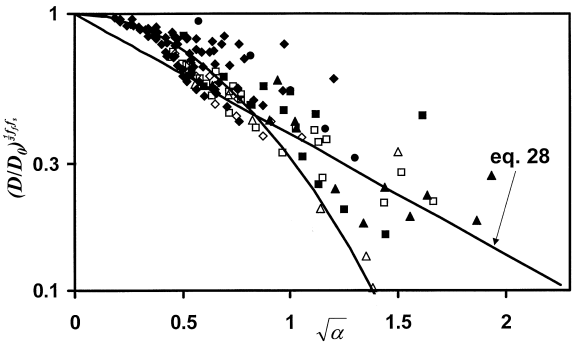

Fig. 7. The fit of Ogston's diffusion model modified with flexibility factors (Eq. (28)); the bent line represents a linear relationship between α and $f_f f_s \ln(D/D_0)$. (For definition of symbols see Fig. 5).

4.4. Two diffusion regimes in Ogston's diffusion model

It is clear in Fig. 7 that at low values of α (<0.7), in structures with little fiber, the theory of Ogston is not correct. Here it appears that $\ln(D/D_0)$ is a linear function of α instead of $\sqrt{\alpha}$. Therefore we propose that the step size in large holes is not limited by the size of the holes but that there is some limiting step size, λ_0, which is related to the solute radius and the fiber radius by a constant, s:

$$\lambda_0 = s(r_s + r_f) \qquad (29)$$

(We think that it would be better justified to relate λ_0 to the solute radius alone, however, this leads to more scatter in the data). The effective step size is then the smallest of the hole size (Eq. (26)) and the limiting step size (Eq. (29)). A convenient empirical formula is:

Table 3
Fitted parameters needed in Eqs. (28) and (31)

$f_{f,agarose}$	1	$f_{s,linear\ polymers}$	2
$f_{f,sephadex}$	1.5	$f_{s,proteins}$	1
$f_{f,polyacrylamide}$	2.25	s	7

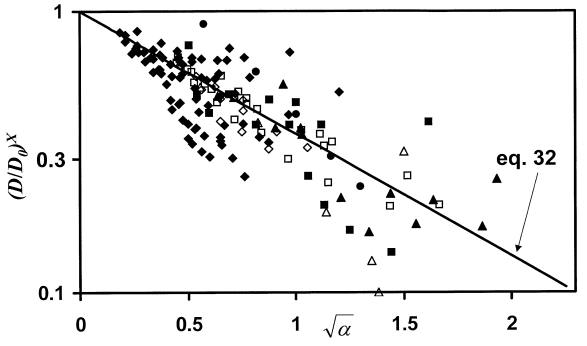

Fig. 8. The fit of Ogston's diffusion model modified with flexibility factors and a maximum step length (Eq. (31)), X on the vertical axis represents:

$$\sqrt{\left(\frac{f_f f_s}{3}\right)^2 + \left(\frac{2}{s}\right)^2 \frac{1}{\alpha}}.$$

(for definition of symbols see Fig. 5).

$$\lambda^{-2} = (s(r_s + r_f))^{-2} + (0.5\sqrt{\pi l})^2 \tag{30}$$

The final result is Eq. (31) and the fit with the data is seen in Fig. 8. The fitted constants are given in Table 3.

$$\frac{D}{D_0} = \exp\left[-\sqrt{\frac{\alpha}{\left(\frac{f_f f_s}{3}\right)^2 + \left(\frac{2}{s}\right)^2 \frac{1}{\alpha}}}\right] \tag{31}$$

The effect of introducing this limiting step size is seen in comparing Figs. 7 and 8 at low α: the fit is much better. The scatter has not changed because the same data points are used.

4.5. Extending Ogston's diffusion model to more complicated systems

We would like to suggest an extension of Eq. (31) to systems with higher concentrations and cosolutes. We propose that α should be replaced by an α_d (subscript d for diffusion), and f_f by an f_d, representing all the objects that can hinder the diffusion. For α_d we propose that one should use the α that one would find for the partitioning at infinite dilution between the bulk and a system of fibers, fixed solutes and fixed cosolutes:

$$\alpha_d = \ln\left(\frac{1}{1 - \phi_f - \phi_i - \sum_j \phi_j}\right) \times \frac{\left(\frac{r_i + r_f}{r_f}\right)^2 \phi_f + 8\phi_i + \sum_j \left(\frac{r_i + r_j}{r_j}\right)^3 \phi_j}{\phi_f + \phi_i + \sum_j \phi_j} \tag{32}$$

For the flexibility factor we propose a weighted average of the flexibility factors. Since obstacles with lower flexibility factors are more important in the retardation we propose:

$$f_d = \frac{\phi_f + \phi_i + \sum_j \phi_j}{\frac{\phi_f}{f_f} + \frac{\phi_i}{f_i} + \sum_j \frac{\phi_j}{f_j}} \tag{33}$$

If there are small non-fixed obstacles among the obstacles, the flexibility factors of these obstacles may have to be increased since they can easily be moved by the solute and therefore offer less resistance to diffusion. Since next to nothing is known about the retardation of diffusion in these complicated systems we are unable to test this extension of the model.

4.6. Discussion

Besides Ogston's diffusion model other models have been proposed that can explain the retardation of diffusion in fibrous structures. In this paragraph we discuss the important ones.

In Ogston's model only the effect of obstruction on the diffusion coefficient is considered. Another model that also incorporates only obstruction effects is the model by Johansson et al. [10]. Their result for stiff fibers (their Eq. (7)) can be approximated closely by:

$$\frac{D}{D_0} = e^{-0.72\alpha} \tag{34}$$

This gives a result comparable to our result for fibrous structures with large holes, although the factor 0.72 is too small. It seems to us that their Eq.

(4), for the retardation in a cylindrical cell, is not valid in fibrous structures with small holes.

It has also been suggested that the additional hydrodynamic friction caused by the fibers can explain the retardation. The fibers around the solute restrict the solvent in its motion, which leads to an increased friction between the solute and the solvent. On this basis Phillips et al. [12] suggested that Brinkman's equation can be used:

$$\frac{D}{D_0} = \left[1 + \sqrt{\frac{r_s^2}{k}} + \frac{r_s^2}{3k} \right]^{-1} \quad (35)$$

where k is the permeability of the fibrous structure. This approach is called the effective medium model. Based on the data collected by Jackson and James [22] k can be estimated by $k = 0.5 r_f^2/\phi$ and it follows that $r_s^2/k \approx 2\alpha$. The equations of Phillips et al. [12] and Ogston et al. [11] then give approximately the same retardation. In this model the effect of fiber flexibility may already be accounted for in the permeability, this is not known. The effect of solute flexibility may be accounted for by changing the effective solute radius.

Finally it has been suggested by Johnson et al. [17] that the retardation by obstruction (Eq. (27)) and by additional friction (Eq. (35)) should be multiplied.

Since Ogston's model, the effective medium model and the multiplication of the results of these two models have approximately the same dependence on α it seems to us that the preference for one of them should be based on their theoretical soundness, on practical considerations (is the permeability known?), or on someones taste. We think Ogston's model is the most elegant one.

Finally it must be said that the results of our own measurements are not very well described by Ogston's models. For the largest protein there is good agreement, but for smaller proteins Ogston's models (with $\phi = 0.06$ and $r_f = 22$ Å, the agarose parameters when there are no ion-exchange groups attached) overestimate the partition and the diffusion coefficient. Apparently the steric effect of the ion-exchange groups is large for small solutes and small for large solutes. However when Eq. (2) and (31) are combined and α is eliminated, giving a relation between K and D/D_0, the agreement is much better.

4.7. Symbols

c	mobile phase concentration, mol/l or g/l
c_{in}	mobile phase concentration coming into a ''tank'', mol/l or g/l
D	diffusion coefficient, m^2/s
D_0	diffusion coefficient in free solution, m^2/s
d_p	particle diameter, m
K	partition coefficient, –
k_l	liquid side mass transfer coefficient, m/s
k_p	particle side mass transfer coefficient, m/s
L	bed length, m
l	fiber length per volume, m^{-2}
L_{tank}	length of a ''tank'', m
MT	mass transfer per particle volume, mol/s m^3
N_A	Avogadro's constant, $6.02 \cdot 10^{23}$ mol^{-1}
q	stagnant phase concentration, mol/m^3
R	gas constant, 8.314 J/mol K
r	sum of radius of fiber and solute ($r = r_f + r_s$), m
T	temperature, K
t_{100}	elution time of peak top, s
$t_{50,\uparrow}$	time at which the eluted peak height is 50 percent of the maximum and peak height is increasing, s
$t_{50,\downarrow}$	time at which the eluted peak height is 50 percent of the maximum and peak height is decreasing, s
v_{sup}	superficial liquid velocity, m/s
α	dimensionless number defined by Eq. (23), –
η	viscosity, $N\,s/m^2$

References

[1] H.A. Sober (Ed.), CRC Handbook of Biochemistry: Selected Data for Molecular Biology, 2nd Edition, The Chemical Rubber Co, Cleveland, OH, 1970.
[2] D.R. Lide (Ed.), CRC Handbook of Chemistry and Physics, 78th Edition, CRC Press, New York, 1997.
[3] P. Vonk, Diffusion of Large Molecules in Porous Structures, Thesis, University of Groningen, 1994
[4] E.J. Wilson, C.J. Geankoplis, I&EC Fundam. 5 (1966) 9.
[5] R. Pfeffer, I&EC Fundamentals 3 (1964) 380.
[6] A.G. Ogston, Trans. Faraday. Soc. 54 (1958) 1754.

[7] L.A. Fanti, E.D. Glandt, J. Colloid Interface Sci. 135 (1990) 396.
[8] B. Amsden, Polymer Gels and Networks 6 (1998) 13.
[9] J.C. Williams Jr., L.A. Mark, S. Eichholtz, Biophys. J. 75 (1998) 493.
[10] L. Johansson, C. Elvingson, J.-E. Löfroth, Macromolecules 24 (1991) 6024.
[11] A.G. Ogston, B.N. Preston, J.D. Wells, Proc. R. Soc. Lond. A. 333 (1973) 297.
[12] R.J. Phillips, W.M. Deen, J.F. Brady, AIChE J. 35 (1989) 1761.
[13] E. Poitevin, P. Wahl, Biophys. Chem. 31 (1988) 247.
[14] M. Moussaoui, M. Benlyas, P. Wahl, J. Chromatogr. 558 (1991) 71.
[15] M. Moussaoui, M. Benlyas, P. Wahl, J. Chromatogr. 591 (1992) 115.
[16] E.M. Johnson, D.A. Berk, R.K. Jain, W.M. Deen, Biophys. J. 68 (1995) 1561.
[17] E.M. Johnson, D.A. Berk, R.K. Jain, W.M. Deen, Biophys. J. 70 (1996) 1017.
[18] J. Tong, J.L. Anderson, Biophys. J. 70 (1996) 1505.
[19] G.K. Ackers, R.L. Steere, Biochim. Biophys. Acta 59 (1962) 137.
[20] T.C. Laurent, J. Killander, J. Chromatogr. 14 (1964) 317.
[21] P.M. Boyer, J.T. Hsu, AIChE J. 38 (1992) 259.
[22] G.W. Jackson, D.F. James, Can. J. Chem. Eng. 64 (1986) 364.